



A novel approach to the study of the development of the Chalk's smectite assemblage

X. F. HU¹, D. LONG² AND C. V. JEANS^{3,*}

¹ Editorial Office, Journal of Palaeogeography, China University of Petroleum (Beijing), 20 Xueyuan Road, P.O. Box 902, Beijing 100083, China, ² Willow View, 46 Litcham Road, Mileham, Norfolk, PE32 2PT, UK, and ³ Department of Geography, University of Cambridge, Downing Place, Cambridge, CB2 3EQ, UK

(Received 30 April 2012; revised 26 July 2013; Editor: Tony Fallick)

ABSTRACT: Detrital, volcanic and diagenetic origins have been used to explain the smectite clay assemblage that characterizes the Upper Cretaceous Chalk of Europe. To further the understanding of how clays of different origins may have converged to this characteristic clay mineral assemblage a new approach is put forward for their investigation. This is based upon (1) the correlation that exists between the trace element and stable isotope geochemistry of the calcite cements preserved within Chalk brachiopods and the various diagenetic phases of early lithification and cementation recognized in the Chalk, and (2) an understanding of the process of late diagenetic cementation that has caused regional differences in the hardness of the Chalk. It is suggested that each phase of lithification and associated calcite cementation may preserve the different clay assemblages at various stages in their convergence to the characteristic Chalk smectite assemblage.

KEYWORDS: Upper Cretaceous, Chalk, lithification, hardgrounds, calcite cement, smectite clays, stable isotopes, trace elements, diagenesis.

The Upper Cretaceous Chalk is a thick (up to 2000 m) and exceptionally pure fine-grained marine limestone that occurs widely in northern Europe. It is the main water, oil and gas reservoir and it is the preferred substrate for many major engineering projects. The Chalk's physical consistency ranges from a soft friable uncemented chalky sediment to a dense fine-grained limestone. The understanding of its nature and properties is of considerable economic and scientific significance. The clay contents and the nature of the clay are particularly important in the development of new Chalk reservoirs and for its engineering properties (Hardman, 1982; Mortimore, 2012). In spite of the important role played by clay minerals, our

knowledge is limited to generalities and restricted qualitative investigations. This reflects not a lack of interest but the inherent difficulties of dealing with the Chalk as a material – the very small size of the clay crystals (generally less than 0.5 μm) and the frequently friable, uncemented and fine-grained nature of the host Chalk which consists predominantly of very fine silt (2–4 μm) and clay-grade (<2 μm) low-magnesium calcite crystals derived from coccoliths, the scales of coccospheres having been secreted by the coccolithophoridae that lived as plankton in the photic zone of the Upper Cretaceous Chalk sea.

THE CHALK SMECTITE QUESTION

Millot (1949) was first to consider that there was something rather special about the clay assemblage in the Chalk. Millot *et al.* (1957), Duplaix *et al.*

* E-mail: CJ302@cam.ac.uk

DOI: 10.1180/claymin.2014.049.2.08

(1960) and Millot (1964) suggested that a montmorillonite-dominated clay assemblage sometimes with a little mica characterized the Chalk of the Paris Basin and was of neoformational origin. Thus the problem of the Chalk montmorillonite was born. In this discussion it will be referred to as the Chalk smectite assemblage. Subsequent research has largely confirmed its widespread nature (Deconinck *et al.*, 2005; Jeans, 2006) except where local detrital sources have contributed kaolin- and mica-rich clay material (e.g. Heim, 1957; Jeans, 2006, fig. 46). Evidence for the neoformational origin is more limited as direct petrographic evidence for the development of the smectite crystals are limited either to studies by transmission electron microscopy that may show euhedral lath-shaped crystal forms as well as evidence of euhedral overgrowths on detrital cores (e.g. Weir & Catt, 1965), or to studies by scanning electron microscopy of silicified patches where bushes of neoformed crystals and opal-CT hemispheres have grown on the walls of pores which have then been coated by a diffuse cloud of very fine clay crystals (e.g. Jeans, 1978). Various authors have suggested that some of the smectite is of volcanic origin, or is detrital derived from smectite-rich soils related to the rising sea levels and water tables as the Upper Cretaceous sea transgressed and drowned low-lying landmasses. There is clear evidence of more or less argillized volcanic ash and phenocrysts (Valeton, 1959, 1960; Schöner, 1960; Dorn & Bräutigam, 1959; Bräutigam, 1962). The argillized volcanic ash is usually in the form of thin marl seams of wide extent, characterized by europium anomalies in their rare earth element patterns (Wray, 1995, 1999; Wray & Wood, 1995, 1998; Wray *et al.*, 1995, 1996). Many other marl seams of wide extent in the Chalk contain no such evidence and are considered to be of detrital origin (Wray & Wood, 1998); however, they could represent the argillization products of unevolved magmas in which europium has not been depleted by its selective uptake in the early crystallization of feldspar. To what extent are the fine euhedral clay laths and overgrowths illustrated by Weir & Catt (1968) the direct precipitate from the dissolution of ash in the porewaters of the sediment is an open question. Deconinck & Chamley (1995) have differentiated between volcanic and detrital smectite in marl seams from the Turonian chalks of northern France based upon their behaviour when heated. Lindgreen *et al.* (2002, 2008) have utilized detailed

structural analysis of the smectite assemblages from the Chalk of Denmark and the North Sea to postulate various sequences of modification related to diagenesis. It is possible that all these origins for the Chalk smectite assemblage have played a role, but it does not answer the question of how the clays from these different sources have ended up as this apparently monotonous and widespread clay assemblage that has characterized the Chalk over the 30–40 Ma years during its deposition and the subsequent 60 million years of diagenesis.

This paper outlines a novel method by which this variation in clay mineralogy can be studied within an independent diagenetic framework by making use of recent advances in the understanding of the cementation and lithification of the Chalk. A similar approach has been used with carbonate nodules (e.g. Raiswell, 1971, 1976; Dickson & Barber, 1976; Hendry *et al.*, 2006) and siliceous nodules (e.g. Jeans 1978; Jeans *et al.*, 1977, 1997) to unravel the sequence of mineral changes that occur during the diagenesis of fine-grained sediments. Sufficient is now known about the cementation and lithification (see Jeans, 1980, p. 82 for use of these terms) in the Cenomanian Chalk of eastern England to treat it as a giant nodule which has developed initially through microbial influence and overpressuring followed by a loss of hydrostatic pressure causing pressure dissolution, the widespread precipitation of a late diagenetic cement, lithification and brittle fracturing. This late calcite cement was responsible for the regional hardening of the Chalk. A subsequent paper in this issue will discuss how the variations and patterns in clay mineral assemblages may be better understood by relating them to the different types and timings of lithification.

The exceptionally fine-grained nature of the Chalk has restricted the direct study of the geochemistry of the cements involved in its lithification in spite of advances in instrumentation (e.g. Maliva & Dickson, 1997). The reason is that sufficiently large crystals of calcite cement are not generally available to determine the history of cementation. Recently this was achieved in the Cenomanian Chalk of eastern England by investigating the calcite cement infilling vugs within the shell cavity of terebratulid brachiopods (Hu *et al.*, 2012). Figure 1 shows such an example. It could be argued that these calcite-filled vugs are the result of allochthonous porefluids that have infiltrated the Chalk at some stage during its diagenesis and have

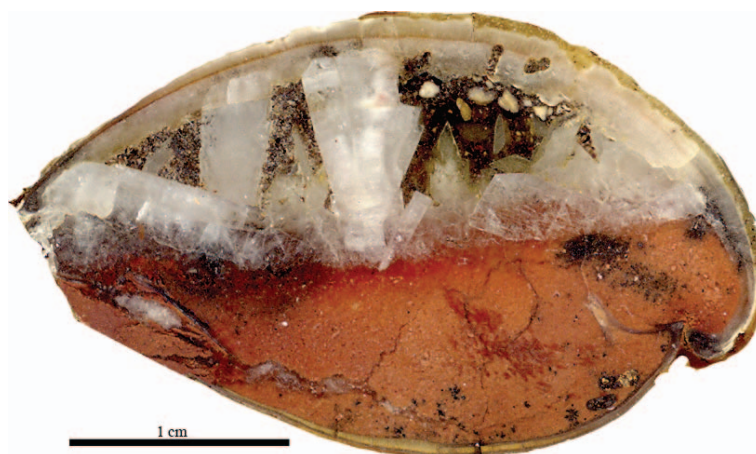


FIG. 1. Baryte and calcite crystals in the shell cavity of brachiopod T1, Belchford Member (Ferriby Formation), Speeton. The best preserved calcite cement forms the roof to the vug. Large crystals of baryte have grown on the chalk floor from solutions rich in sulfate and barium at the margin of the sulfidization zone that cuts across the pink and red bands in the Ferriby Formation.

managed to penetrate the well preserved brachiopods with their tightly fitting valves. However, evidence outlined below demonstrates that the calcite infillings are the result of precipitation from the Chalk's autochthonous pore waters. The pattern of trace elements in the calcite cement in the vugs can be matched with the bulk geochemistry of different types of lithification in the main mass of the Chalk. This will be discussed in more detail later in this paper.

Locations mentioned in the text are shown in Fig. 2. Stratigraphical terms used in the description of the Cenomanian Chalk of eastern England are shown in Fig. 3. Sample horizons are shown in Fig. 4 (Speeton) and Fig. 5 (Hunstanton and Stenigot).

GEOCHEMISTRY OF THE BRACHIOPOD CALCITE CEMENT

The calcite-filled vugs preserved in these terebratulid brachiopods are probably associated with individuals that had been buried alive within the chalk sediment. In such circumstances their valves would have been tightly shut and it was only after death when the musculature holding the valves together started to decompose that some sediment found its way into the body cavity leaving a considerable pore-fluid filled void into which grew large crystals of calcite cement. Cathodoluminescent imagery, staining, electron microprobe

and stable isotope analysis of polished sections (methods of analysis are given in Hu *et al.*, 2012) show that the calcite crystals preserve a record of the geochemistry of the cements which is related to the early diagenesis of the chalk sediment. Figure 6a,b shows the cathodoluminescent imagery from brachiopod T1 (also see Fig. 1).

Two well defined patterns of calcite cementation based on their geochemistry are recognized. The suboxic series is associated with brachiopods from the coloured chalks at Speeton (Fig. 7) which contain a fine-grained hematite pigment (its precursor is assumed to be $\text{Fe}(\text{OH})_3$). This displays a pattern (Fig. 8) starting with Mg-rich, followed by Mn-rich and finally Fe-rich cements with increasingly high $\delta^{13}\text{C}$ values. The other cement pattern, the anoxic series, is found in brachiopods associated with the development of glauconite-stained submarine hardgrounds from chalks that originally contained the precursor $\text{Fe}(\text{OH})_3$ but no longer do so. The trace element pattern is distinctive (Fig. 9) starting with a Mg-rich phase (zone A) followed by zones (B-F) enriched in Mn showing antipathetic variations in Fe and Mn, then zones (F to H) dominated equally by Fe and Mn – the youngest zones (I, J) have very low concentrations of trace elements. Carbon isotope values become increasingly negative as cementation progressed. Figure 10 summarizes the relationship between these two patterns and how they are related to the early lithification of the chalk sediment (Hu *et al.*, 2012).

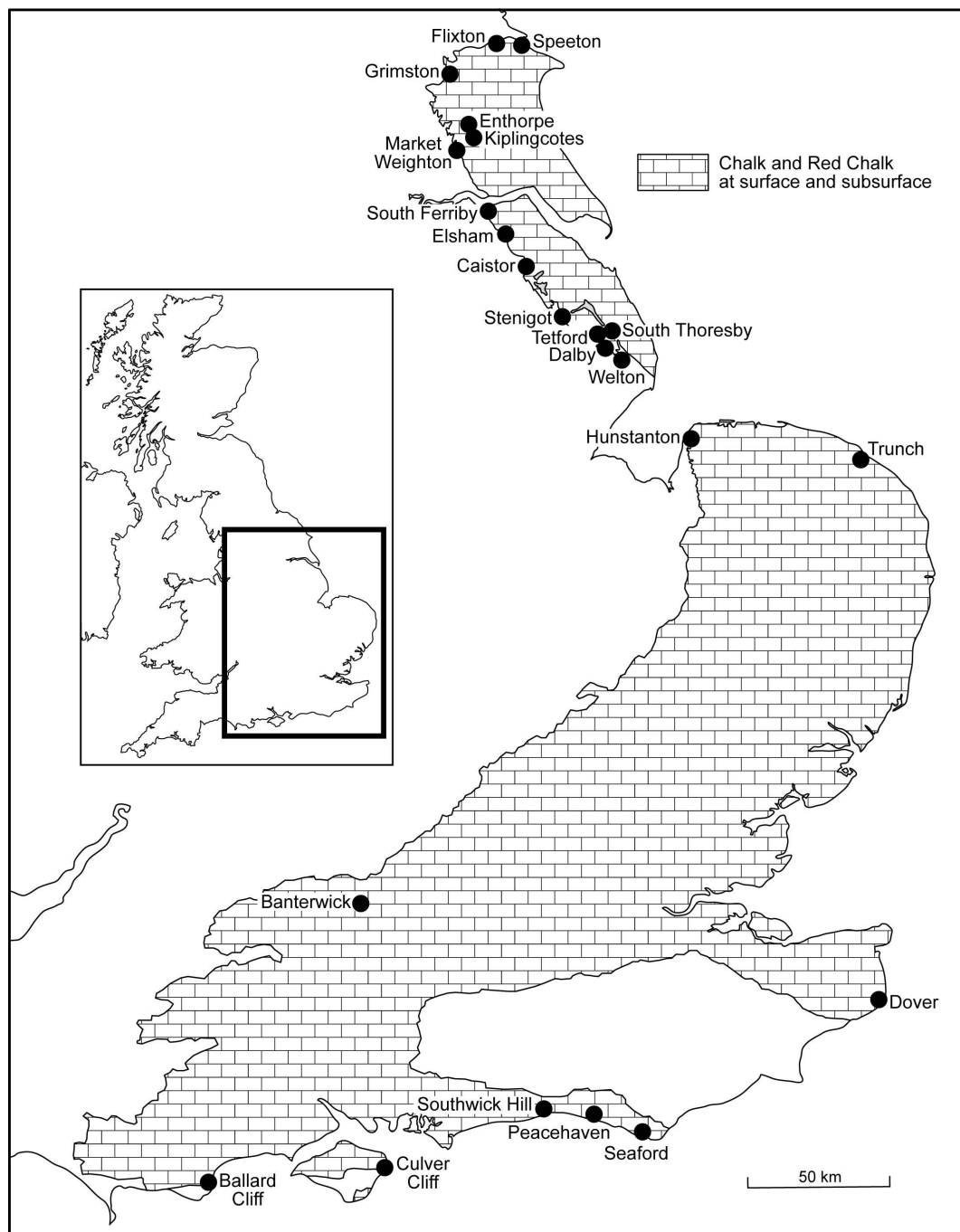


FIG. 2. Distribution of the Upper Cretaceous Chalk and the Upper Albian Red Chalk in the UK showing locations mentioned in the text. The Red Chalk is restricted to Hunstanton and the area to the north.

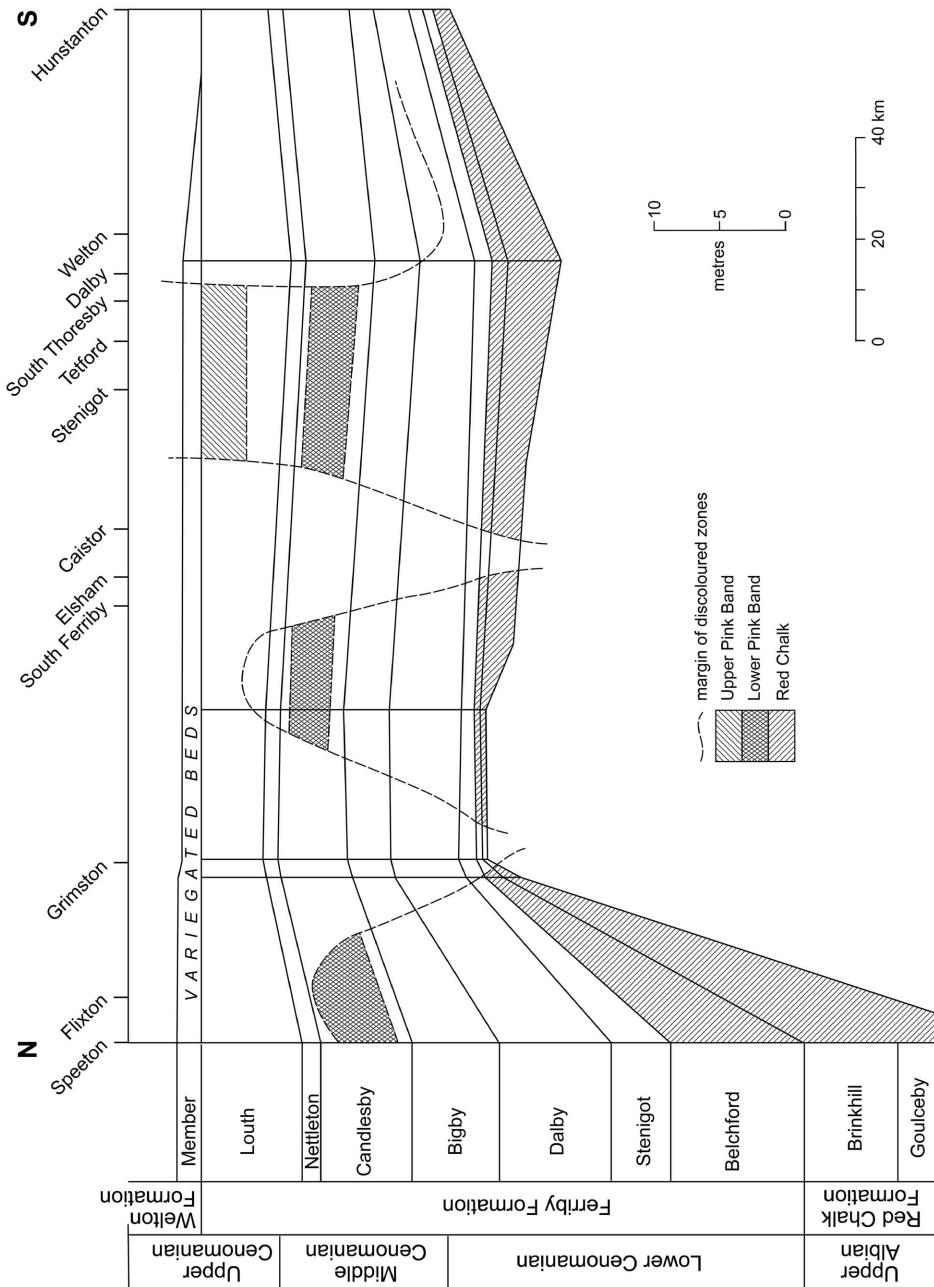


FIG. 3. Horizontal section of eastern England showing the overall stratigraphy of the Late Albian Red Chalk Formation, the Cenomanian Ferriby Chalk Formation and the Turonian Welton Chalk Formation in relation to the general distribution of red colouration. The subdivision into members is based on Jeans (1980), the upper and lower pink bands are those of Bower & Farmery (1910). The formational terms are those of Wood & Smith (1978).

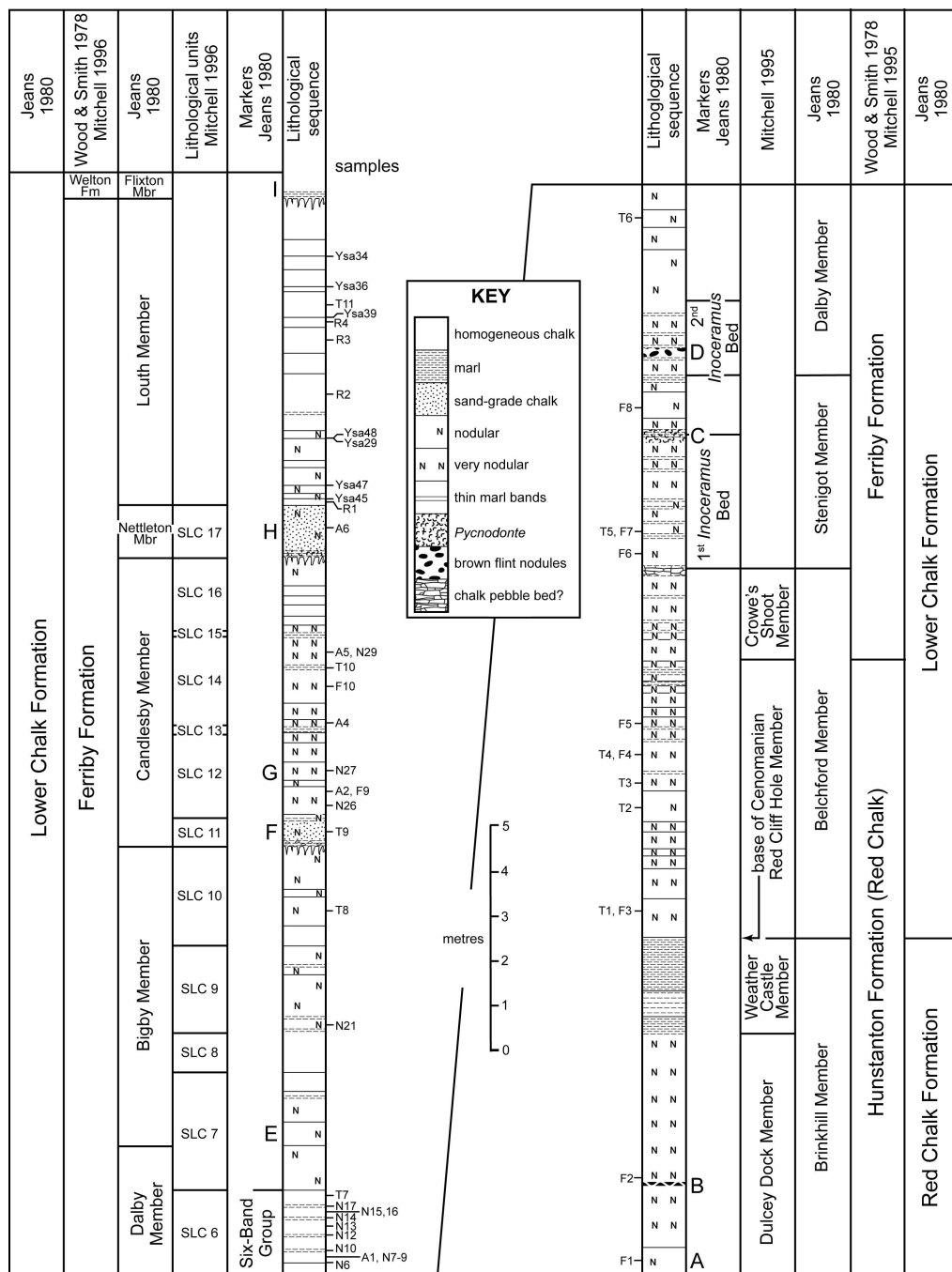


FIG. 4. Lithostratigraphy of the upper part of the Red Chalk Formation and the Ferriby Formation at Speeton, Yorkshire, based upon Jeans (1980, fig. 16). (A) *Inoceramus*-rich horizon. (B) Breccia-nodule Band. (C) Band of abundant *Pycnodonte*. (D) Brown Flint Band. (E) Lower *Orbirhynchia* Band. (F) Grey Bed. (G) Upper *Orbirhynchia* Band. (H) Nettleton Stone. (I) Variegated Beds. Horizons of the terebratulid brachiopods (T1–T11) described in detail by Hu *et al.* (2012) and other samples mentioned in this investigation are indicated. The various schemes of lithological subdivisions used by Mitchell (1995, 1996) are shown.

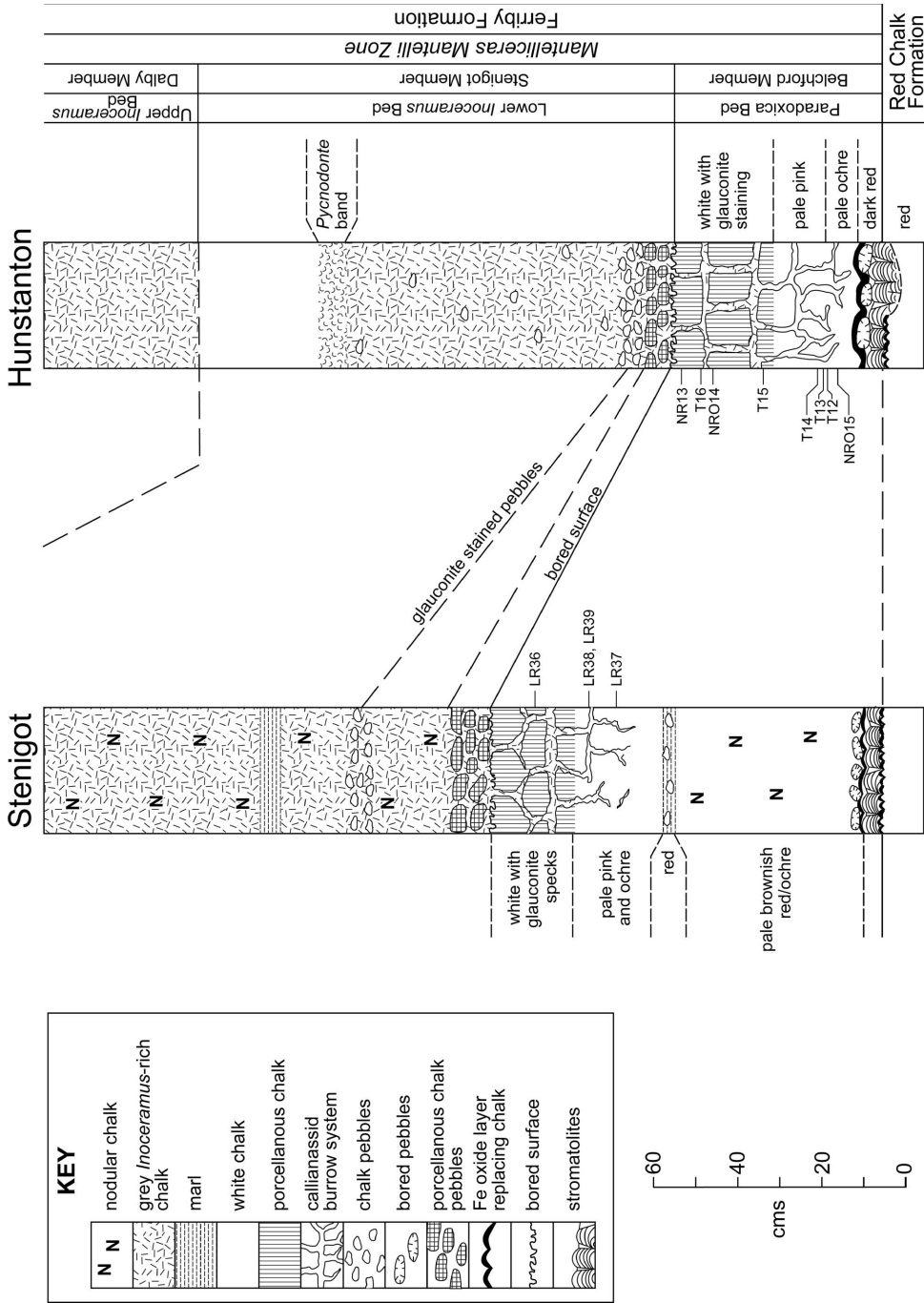


Fig. 5. The lithostratigraphy of the basal part of the Ferraby Formation at Hunstanton (Norfolk) and Stenigot (Lincolnshire). Horizons of terebratulids T12–T16 and other samples are indicated.

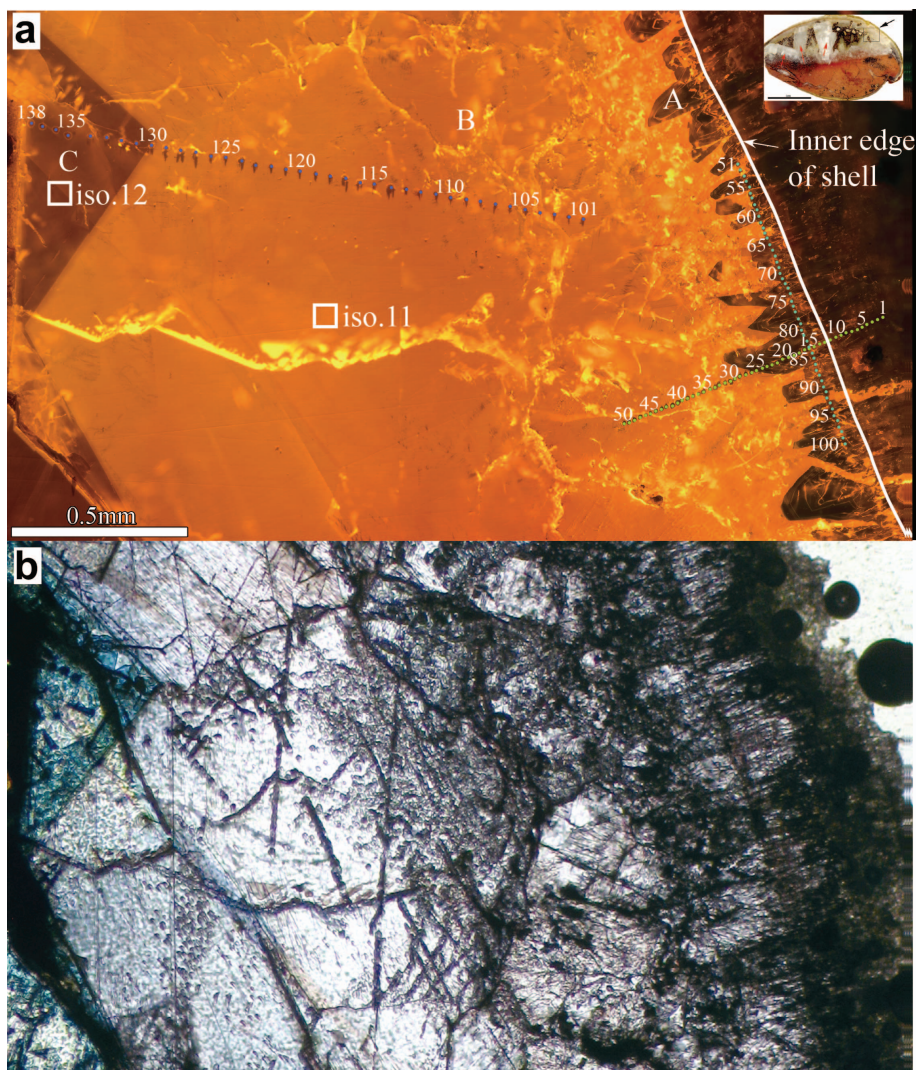


FIG. 6. (a) CL image of calcite cement in brachiopod T1. Zone A consisting of non-luminescent crystals (enriched in Mg) attached to the inner wall of the ventral valve. Zone B is bright orange and is Mn-rich. Zone C is dull orange and is Fe-rich. The transects of EMPA (1–138) are clearly seen, the locations of isotope analyses are shown – the data are given in Hu *et al.* (2012). (b) The same field of view as Fig. 6a but under plane-polarized light and stained. Zone B stains as non-ferroan calcite (pink), Zone C stains as ferroan calcite (blue).

CHALK LITHIFICATION AND ITS RELATIONSHIP TO THE BRACHIOPOD CEMENT STRATIGRAPHY

In order to use the brachiopod cement stratigraphy to establish the diagenetic development of the smectite clay assemblage it is necessary to show that the various phases of lithification recognized

by Jeans (1980) in the Cenomanian Chalk in eastern England and the Campanian Chalk at Peacehaven in Sussex can be related to what has been observed in the brachiopods. Only then is there a basis to obtain samples for clay mineral analysis that will reflect this diagenetic framework.

Four different types of early lithification have been recognized by their field occurrence and Fe



FIG. 7. Red and pink nodular chalks of the Belchford Member at the base of the Cenomanian Chalk at Speeton. The blue/grey nodular chalk at the base has resulted from the reduction of the hematite pigment with the development of pyrite and marcasite crystals during late diagenesis (Jeans, 1973). Scale 105 mm \times 150 mm.

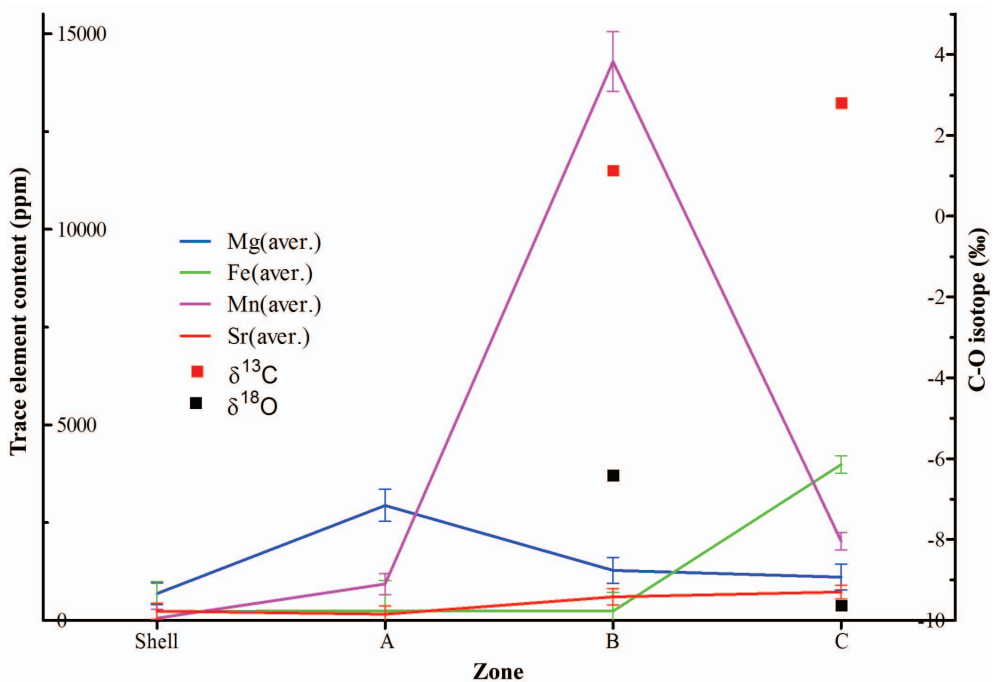


FIG. 8. Average trace element zonal values and isotope values (VPDB) arranged along the direction of crystal growth for the typical example (terebratulid brachiopod T1) of suboxic cementation from Speeton (Hu *et al.*, 2012, fig. 20).

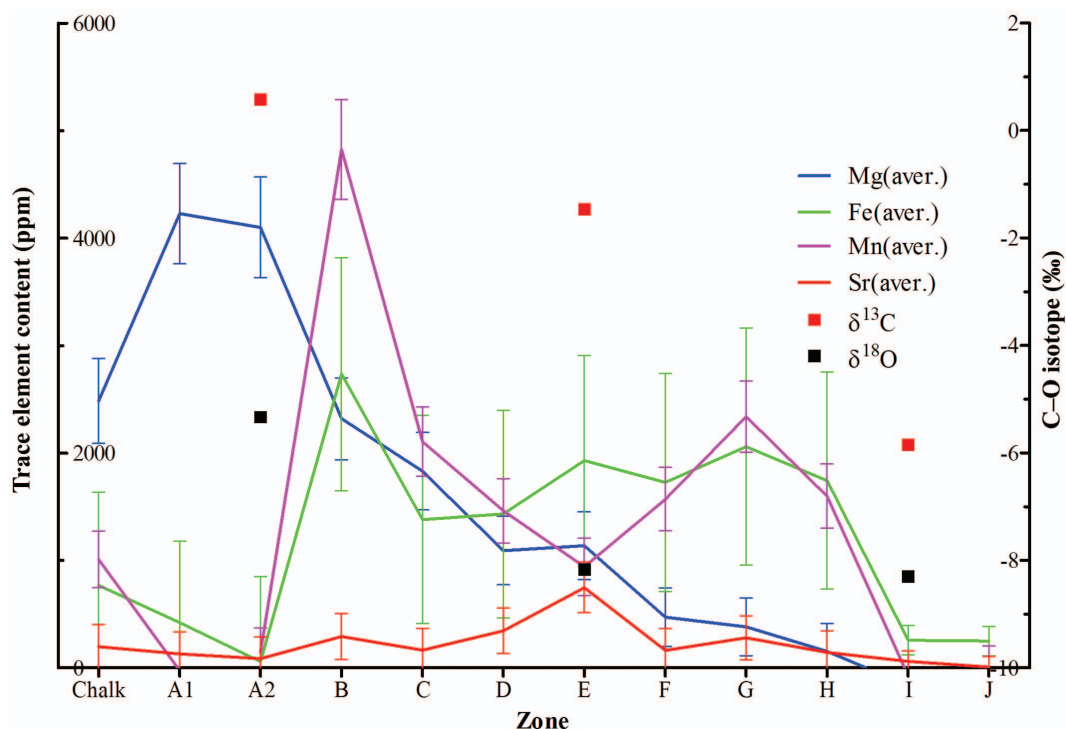


FIG. 9. Average trace element zonal values and isotope values (VPDB) arranged along the direction of crystal growth for the typical example (combined data from brachiopods T12–T16) of anoxic cementation from Hunstanton (Hu *et al.*, 2012, fig. 21).

geochemistry of their bulk calcite in the Cenomanian Chalk of eastern England (Jeans, 1980). A late diagenetic lithification was also identified in this Chalk where it had not been affected by early lithification – this was related to regional pressure dissolution. Additional trace element (Fe, Mn, Mg, Sr) and stable isotope ($\delta^{18}\text{O}$ and $\delta^{13}\text{C}$) analysis of the bulk calcite of chalks affected by these different types of lithification have been carried out using the methods described in Jeans *et al.* (1991, 2012) in order to identify (a) the geochemical fingerprint of their cements above the background composition of the original bioclastic material, and (b) similarities with the pattern of trace elements found in the calcite filled vugs of the brachiopods.

Large ammonites at Speeton (Jeans, 1980, Type 4 lithification)

The preferential calcite cementation associated with large ammonites preserved in the nodular chalks is considered to represent the earliest

lithification as it is related to what must have been their rotting remains within their aragonite shell buried in the chalk sediment. There is, however, no systematic difference in the stable isotope values between the ammonites and their nodular chalk surrounds (Jeans *et al.*, 2012, table 4). Table 1 contrasts the trace element concentrations of the bulk calcite associated with a number of large ammonites with that of the surrounding nodular chalk. The ammonite calcite displays enhanced values of Mg and Mn relative to the nodules, and also of Fe relative to the matrix of their nodular surrounds. Comparison to the suboxic pattern of cementation indicates that the Mg-rich, Mn-rich and Fe-rich phases of brachiopod cement are represented.

Nodular chalks at Speeton (Jeans, 1980, Type 5 lithification)

Nodular chalks are a major component of the Red Chalk and Ferriby formations at Speeton (Fig. 4). Jeans *et al.* (2012, table 5) have shown that there are

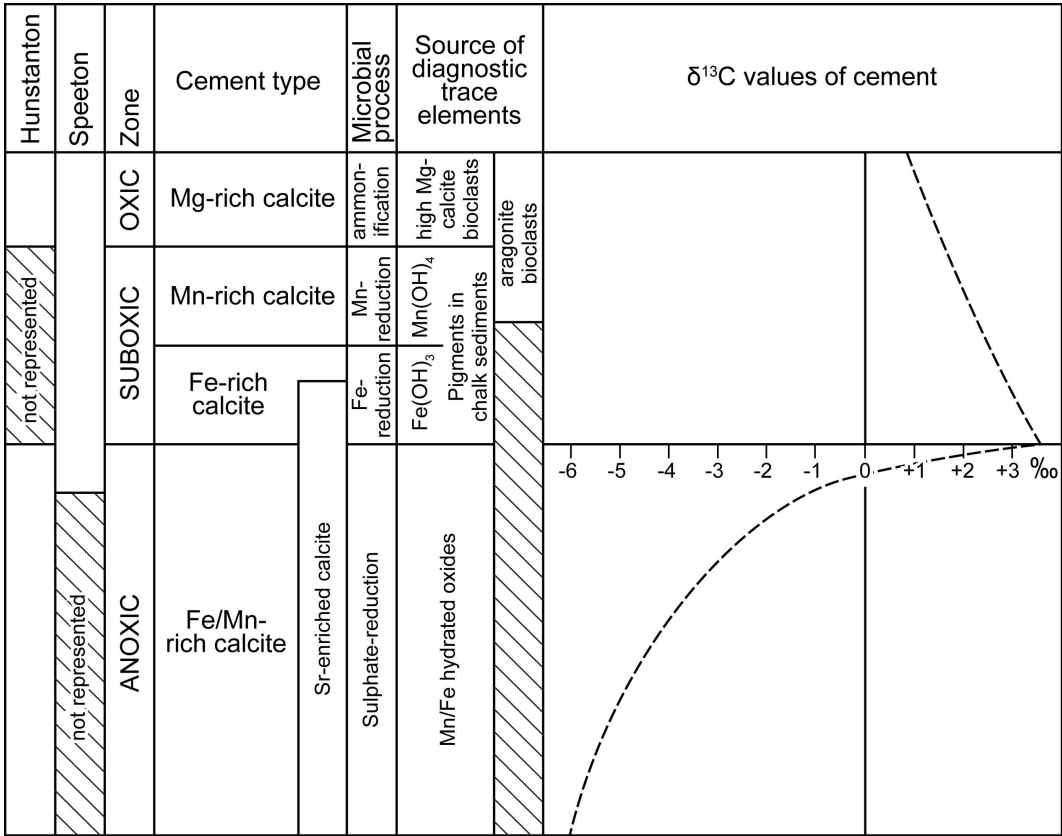


FIG. 10. Schematic diagram summarizing the interpretation of the suboxic and anoxic cement series (Hu *et al.*, 2012, fig. 27).

no systematic differences in the stable isotope values between the bulk calcite from the nodules and matrices making up the nodular chalks. Tables 2 and 3 contrast the trace element contents of the bulk calcite in two series of nodular chalk from different members of the Ferriby Formation at Speeton. The Fe content of the nodule calcite is always enhanced relative to the matrix, whereas the Mg and Mn contents show no consistent pattern. Comparison to the suboxic pattern suggests that this early cementation represents only the late Fe-rich phase in the brachiopod cement and was not affected by the earlier Mg- and Mn-enriched cements.

Late lithification associated with pressure solution cements at Speeton

At Speeton, regional cementation due to pressure solution has been shown to postdate the completion of suboxic cementation (Hu *et al.*, 2012). Table 4

shows the $\delta^{18}\text{O}$ and $\delta^{13}\text{C}$ values of the residual calcite from a series of pressure dissolution marl seams and the bulk calcite of the adjacent beds of chalk in the Louth Member (Ferriby Formation). The marl seams not only have considerably higher acid insoluble residues but they have higher $\delta^{18}\text{O}$ and $\delta^{13}\text{C}$ values. The values from the marl seams are considered to represent the original chalk bioclasts without addition of any calcite cement; however, the original bulk $\delta^{13}\text{C}$ value has been modified by the selective pressure dissolution of the finest calcite fraction (<2 μm) consisting of coccolith crystals which usually have lower $\delta^{13}\text{C}$ values than bioclastic material (Jeans *et al.*, 1991, fig. 8). The lower $\delta^{13}\text{C}$ values in the chalk beds reflect the inheritance of the coccolith HCO_3^- from the marl seams, whereas the lower $\delta^{18}\text{O}$ values suggest an enhanced temperature of cementation. This late-stage cementation will therefore display a $\delta^{13}\text{C}$ trend towards more negative values.

TABLE 1. Calcite trace elements associated with large ammonites (Type 4 early lithification) in the Cenomanian Chalk, Speeton. Sample horizons in Jeans (1980, fig. 16); ammonites A7 (red, grey) are from the same stratigraphical level as A3.

Ammonite no.	Ammonite interior (AI)/Nodule interior (NI)	— CaCO ₃ — Wt.%	— Fe (calcite) — AI/NI	— Mn (calcite) — AI/NI	— Mg (calcite) — AI/NI	— Sr (calcite) — AI/NI	
			ppm	ppm	ppm	ppm	
A6	AI	98	1.03	1.04	1.38	371	0.86
	NI	95		1061	1829	431	
A5	AI	96	1.03	0.98	1.38	2209	1.20
	NI	93		612	1835	459	0.84
	matrix	93	—	320	1300	2049	—
A4	AI	94	1.00	1.00	1.15	2141	1.12
	NI	94		701	1359	465	0.93
A2	AI	95.6	0.98	1.19	1.21	2197	1.05
	NI	97.7		450	1350	368	0.96
	matrix	72.2	—	150	1628	2997	—
A7 (red)	AI	95	1.00	0.89	1.12	2296	1.23
	NI	95		597	1227	416	0.89
A7 (grey)	AI	95	1.00	1.02	1.43	2497	1.34
	NI	95		570	1184	396	0.51
	matrix	56	—	125	1729	3048	—
A1	AI	95	1.00	0.92	1.03	2117	1.19
	NI	95		622	1252	368	0.94
	matrix	56	—	125	1729	392	—
						310	—



FIG. 11. General view of the cliffs at Hunstanton showing the Carstone (Middle to Lower Albian; brown limonitized berthierinitic sandstone) passing up into the Red Chalk Formation (Upper Albian) which is overlain by greyish white Cenomanian chalk of the Ferriby Formation. The conspicuous white bed at the base of the Chalk is the Paradoxica Bed hardground.

Paradoxica Bed hardground at Hunstanton
(Jeans, 1980, Type 1 lithification)

The development of this hardground lithification (Fig. 11) reflects a regional event, in this instance the whole area of the East Midland Shelf from north Norfolk to south Yorkshire (Fig. 3). The

hardground is related to a long established surface of nil or negative deposition marking the top of the Belchford Member of the Ferriby Formation that affected the underlying chalks containing $\text{Fe}(\text{OH})_3$, the precursor to the hematite pigment responsible for the red or pink colouration of much of the

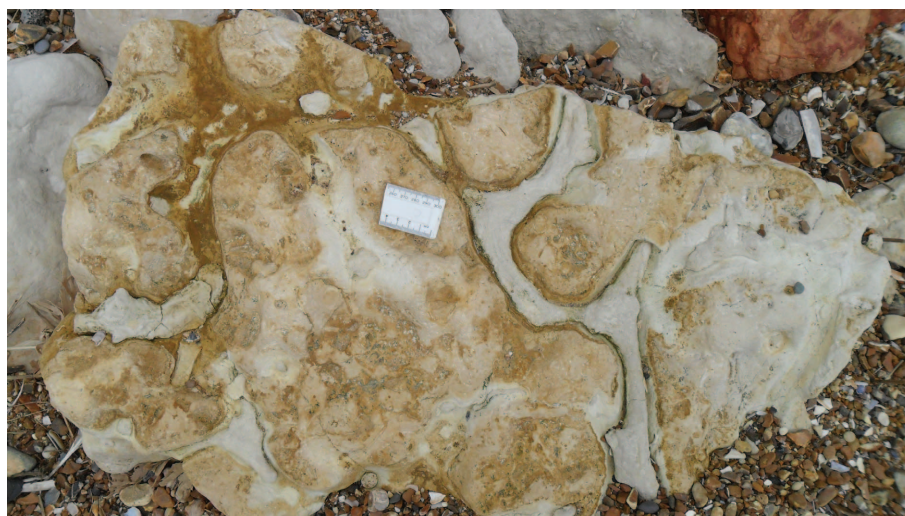


FIG. 12. Fallen block of the Paradoxica Bed hardground with callianassid burrows with glauconite-stained walls which are filled with chalk.

TABLE 2. Calcite trace elements in nodular chalks and marls in the Cenomanian Chalk, Speeton (Type-5 early lithification). Sample horizons in Fig. 4.

Sample no.	Nodule/matrix	Wt.% CaCO ₃	N/M	– Fe (calcite) – ppm	N/M	– Mn (calcite) – ppm	N/M	– Mg (calcite) – ppm	N/M	– Sr (calcite) – ppm	N/M
N29	nodule (N) matrix (M)	90 78	1.15	525 320	1.64	1580 1300	1.22	1350 2049	0.66	515 428	1.20
F10	nodule (N) matrix (M)	82.4 80.8	1.02	252 150	1.68	1694 1729	0.98	1915 1649	1.16	539 485	1.11
N28	nodule (N) matrix (M)	98 66	1.48	545 200	2.73	1460 1299	1.12	1350 1851	0.73	428 405	1.06
N27	nodule (N) matrix (M)	95 82	1.16	470 258	1.82	1460 1621	0.90	1450 2000	0.73	390 338	1.15
A3	nodule (N) matrix (M)	96 80	1.20	500 325	1.54	1340 1580	0.85	1859 2401	0.77	365 405	0.90
F9	nodule (N) matrix (M)	97.7 72.2	1.35	450 150	3.00	1350 1628	0.83	2100 2997	0.70	368 353	1.04
N26	nodule (N) matrix (M)	94 85	1.11	579 333	1.74	1381 1521	0.91	1601 2151	0.74	388 390	0.99
N17	nodule (N) matrix (M)	93 53	1.75	583 93	6.27	1180 1520	0.78	1600 3500	0.46	385 285	1.35
N15-16	nodule (N) matrix (M)	94 61	1.54	545 233	2.34	1340 1960	0.68	1600 2825	0.57	355 310	1.15
N14	nodule (N) matrix (M)	93 74	1.26	463 195	2.37	1240 1580	0.78	1750 2500	0.70	375 338	1.11
N13	nodule (N) matrix (M)	94 64	1.47	483 133	3.63	1240 1469	0.84	1600 3093	0.52	410 334	1.23
N12	nodule (N) matrix (M)	94 52	1.81	465 93	5.00	1120 1800	0.62	1800 3324	0.54	428 338	1.27
N10	nodule (N) matrix (M)	93 63	1.48	470 162	2.90	1298 1730	0.75	1748 3199	0.55	373 300	1.24
N7-9	nodule (N) matrix (M)	94 56	1.68	495 125	3.96	1300 1729	0.75	1600 3048	0.52	375 310	1.21
N6	nodule (N) matrix (M)	94 59	1.59	500 125	4.00	1299 2170	0.60	2049 3300	0.62	405 285	1.42
F8	nodule (N)	91.3	1.57	612	2.28	1920	0.78	1800	0.58	403	0.96

F7	matrix (M)	58.2	1.22	269	1.50	2448	0.76	3097	418	0.86
	nodule (N)	90.4		487		2000		2500	403	
	matrix (M)	74.2		325		2630		2950	468	
F6	nodule (N)	93.9	1.17	575	1.44	2030	0.70	2350	403	0.94
	matrix (M)	80.2		400		2900		2600	430	
F5	nodule (N)	86.8	1.36	450	1.72	2598	0.70	2348	535	0.97
	matrix (M)	63.7		262		3695		2247	549	
F4	nodule (N)	86.9	1.18	474	1.95	3074	1.09	2295	664	1.17
	matrix (M)	73.5		243		2818		2235	567	
F3	nodule (N)	88.6	1.32	512	2.06	1949	0.89	2149	450	1.00
	matrix (M)	66.9		249		2195		2894	449	
F2	nodule (N)	84.3	1.89	425	2.35	2928	1.41	2498	450	0.61
	matrix (M)	44.7		181		2080		2600	735	
F1	nodule (N)	89.5	1.21	568	1.11	2298	0.89	2698	335	0.80
	matrix (M)	74		512		2578		2498	418	

Cenomanian Chalk in eastern England (Fig. 7). The sediment underlying the surface was extensively colonized and bioturbated by an infauna, the $\text{Fe}(\text{OH})_3$ having been lost and all the surfaces of the resulting Paradoxica Bed hardground that were in contact with ambient seawater are stained with glauconite (Fig. 12). The development of anoxic conditions, cementation and dissolution of the $\text{Fe}(\text{OH})_3$ took place while the sediment was penetrated by an open reticulate system of branching burrows occupied by callianassid crustaceans (Jeans, 1980, fig. 9). The trace element chemistry of the bulk calcite from different levels within the Paradoxica Bed at Hunstanton and Stenigot is shown in Table 5. The enrichment in Mg towards the top surface of the bed at Hunstanton is noteworthy, probably reflecting the increasing amount of the early Mg-enriched cement that is seen in brachiopods T12–T16 (Fig. 9).

Incipient hardgrounds, Campanian Chalk, Peacehaven, Sussex

Another variety of early regional lithification which is related to anoxic calcite cementation occurs at a much higher stratigraphical level in the Chalk of southern England. It may be much more widespread both stratigraphically and regionally, but this is uncertain as it is not readily identifiable in the field. This is known from the sequence of variably cemented white chalk with flints and thin marl seams of Campanian age (stratigraphical details are shown in Jeans *et al.*, 2012, fig. 13) exposed at the Peacehaven Steps Cliff section on the Sussex coast (Fig. 13). There is no evidence of hardground development or of glauconite staining. Rusty patches and stains to fossils suggest the former presence of iron sulfides. Stable isotope analysis of the bulk calcite of 65 samples collected at 25 cm interval shows covariation between the $\delta^{18}\text{O}$ and $\delta^{13}\text{C}$ values (Fig. 14), suggesting that two end-member chalks of different stable isotope composition were involved, one with relatively high $\delta^{18}\text{O}$ and $\delta^{13}\text{C}$ values, the other with lower values. Further investigation (Jeans *et al.*, 2012) has confirmed this. Very little difference was present in the $\delta^{18}\text{O}$ and $\delta^{13}\text{C}$ values of the separated sand (>63 μm) and silt fractions (2–63 μm) whereas the <2 μm fraction $\delta^{18}\text{O}$ values ranged from –2.0 to –5.4‰ and $\delta^{13}\text{C}$ values from 1.4 to –8.3‰. The <2 μm fraction of the topmost thirteen samples (PHS53–PHS65) from the section were also analysed but displayed $\delta^{18}\text{O}$

TABLE 3. Calcite trace elements in red nodular chalk, Dulcey Dock Member, Red Chalk Formation, Speeton (Fig. 4).

Sample no.	Nodule/ matrix	CaCO ₃		Fe (calcite)		Mn (calcite)		Mg (calcite)		Sr (calcite)	
		Wt.%	N/M	ppm	N/M	ppm	N/M	ppm	N/M	ppm	N/M
Grp B/1/1	nodule (N)	91	1.25	270	1.80	2950	0.90	2000	1.21	507	0.97
	matrix (M)	73		150		3280		1650		525	
Grp B/1/2	nodule (N)	95	1.36	270	1.80	2920	0.83	1750	0.97	480	0.96
	matrix (M)	70		150		3500		1800		500	
Grp B/1/3	nodule (N)	89	1.41	245	2.04	3598	1.15	1999	0.98	373	0.75
	matrix (M)	63		120		3120		2050		500	
Grp B/1/4	nodule (N)	—	—	—	—	—	—	—	—	—	—
	matrix (M)	56		75		3098		2399		480	
Grp B/1/5	nodule (N)	90	1.30	275	2.46	3001	0.94	1850	0.93	465	1.04
	matrix (M)	69		112		3198		1999		445	
Grp B/1/6	nodule (N)	91	1.25	242	2.60	3278	0.91	1849	1.06	445	0.86
	matrix (M)	73		93		3600		1750		520	
Grp B/1/7	nodule (N)	91	1.30	242	2.02	3118	1.03	1849	1.06	475	0.88
	matrix (M)	70		120		3029		1750		540	
Grp B/1/8	nodule (N)	87	1.30	163	1.44	3030	1.09	1850	0.90	480	0.90
	matrix (M)	67		113		2770		2050		535	

TABLE 4. Stable isotope values (VPDB) associated with chalk beds and pressure solution marls, Louth Member (Ferriby Formation), Speeton. Sample horizons in Fig. 4.

Sample no.	CaCO ₃ (wt.%)	δ ¹³ C (‰)	δ ¹⁸ O (‰)
R11	91	3.05	-4.37
R12	90	2.99	-4.3
Ysa34	59	3.18	-2.8
R13	90	2.95	-4.35
R13	90	2.95	-4.35
Ysa36	61	3.13	-2.09
R4	92	3.02	-4.6
R4	92	3.02	-4.6
Ysa39	49	3.14	-2.68
R3	99	2.94	-4.69
R9	89	2.93	-4.85
Ysa48	51	3.15	-3.39
Ysa29	54	3.14	-3.67
R8	87	2.82	4.55
R6	91	2.75	-4.18
Ysa47	50	3.15	-2.69
R1	95	2.86	-3.93
Ysa45	50	3.07	-3.33

R: chalk bed; Ysa: marl seam

TABLE 5. Calcite trace elements in the Paradoxica Bed hardground at Hunstanton and Stenigot. Sample horizons in Fig. 5.

Horizon and location	CaCO ₃ (wt.%)	Fe (calcite) (ppm)	Mn (calcite) (ppm)	Mg (calcite) (ppm)	Sr (calcite) (ppm)
Paradoxica Bed, Belchford Member, Ferriby Formation, Hunstanton					
Upper part (NR13)	95	295	1159	2299	250
100 mm below top surface (NR14)	96	307	1159	1873	280
400 mm below top surface (NR15)	94	490	1600	1400	363
Paradoxica Bed, Belchford Member, Ferriby Formation, Stenigot					
Upper part (LR36)	96	273	1330	2250	225
Middle part (LR38)	90	213	1090	2751	257
Middle part (LR39)	93	112	999	2922	232
Lower part (LR37)	97	197	959	2573	250

(−1.7 to −2.0‰) and $\delta^{13}\text{C}$ (1.6 to 2.3‰) values no different from the bulk. Figure 15 is a $\delta^{18}\text{O}/\delta^{13}\text{C}$ cross plot on which all the analyses from the bulk chalk and the <2 μm fractions have been plotted. It demonstrates that the isotopic covariance originally noted is the result of varying mixtures of normal chalk ($\delta^{18}\text{O}$, −1.5 to −2.5‰; $\delta^{13}\text{C}$, 2.5‰) with a fine-grained cement with approximate values of $\delta^{18}\text{O}$ −8‰ and $\delta^{13}\text{C}$ −8‰.

CONCLUSIONS

The identification of different phases of lithification within the Chalk and the geochemistry of their calcite cements provides a basis by which various stages in the development of the smectite clay assemblage can be investigated. This is summarized in Fig. 16.



FIG. 13. Low-angle aerial photograph of the zig-zag steps cut into the cliff of Campanian chalk at Peacehaven, Sussex. The section between the Old Norse Marl (ONM) and the Castle Hill Marl (CHM) was sampled. Stratigraphy based on Mortimore (1986). MP is the Meeching Marl Pair.

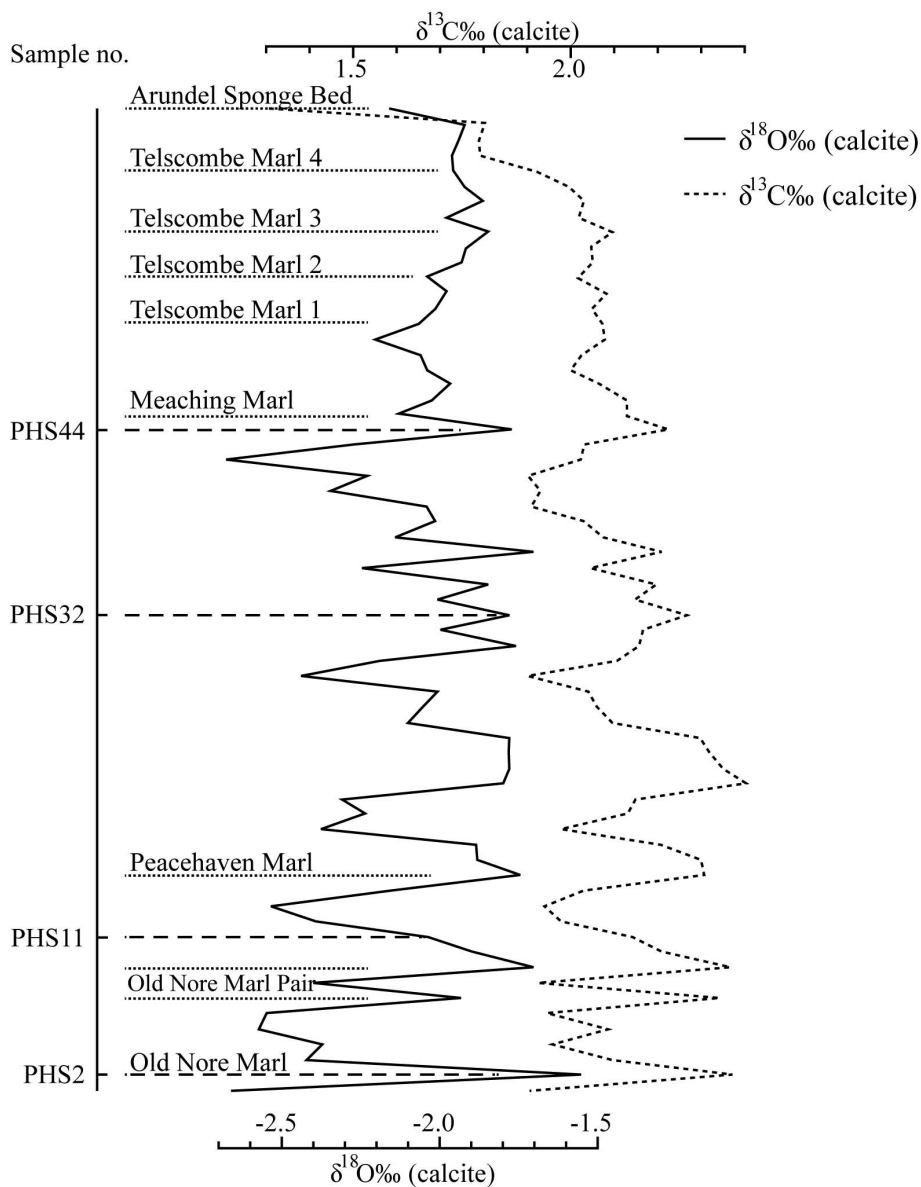


FIG. 14. Stratigraphical variation in the stable isotope values (VPDB) of 65 bulk chalk samples from the Lower Campanian section at Peacehaven Steps, Sussex.

Suboxic cementation

At Speeton, where chalk deposition was essentially continuous and reactions between ambient seawater and the contents of the sediment must have been minimal, five different stages of diagenesis can be used as a time framework to investigate the variation in the smectite assemblage. The earliest stage in the evolution of the smectite

assemblage may be preserved in the chalk associated with large ammonites where the full pattern of suboxic cementation is retained. The next stage is that associated with the nodules in nodular chalks which display only the final Fe-rich phase of cementation. A later stage in the development of this assemblage at Speeton may be reflected in the sediment little affected by early cement but

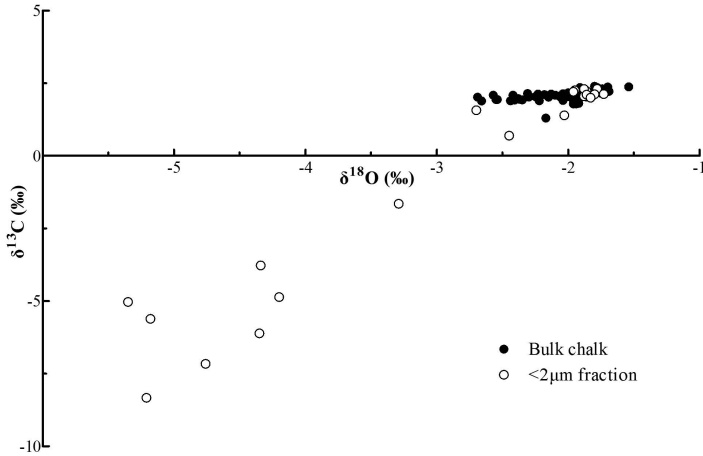


FIG. 15. Cross plot of stable isotope values (VPDB) of 65 bulk chalk samples and the <2 μm fractions of 23 chalk samples from Peacehaven Steps, Sussex.

influenced by the movement of compaction pore waters migrating upwards. A further stage could be preserved in the chalk unaffected by early

lithification but which underwent an extended phase of overpressuring before being cemented and lithified by pressure dissolution. An even later

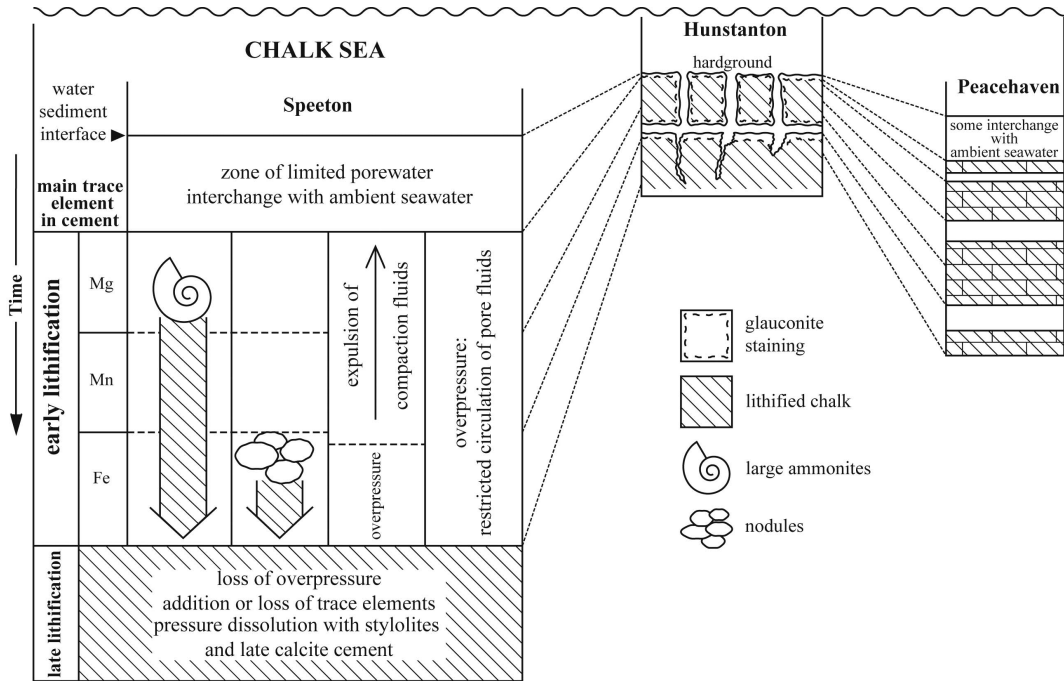


FIG. 16. Scheme of diagenesis showing the different stages in the development of lithification, overpressure and pressure dissolution at Speeton (Yorkshire) in relation to the formation of the hardground at Hunstanton (Norfolk) and incipient hardgrounds at Peacehaven Steps (Sussex). It is suggested that these stages can be used to further the investigation of the development of the Chalk's smectite assemblage as the calcite cementation restricts access to diagenetically later pore fluids.

phase may be recorded in the differences that are present between the pressure dissolution marl seams and the adjacent chalk undergoing regional calcite cementation.

Anoxic cementation

The Paradoxica Bed hardground and its crustacean burrow system is likely to reveal more about the original clay assemblage at the time of deposition and how this has been modified by the long-term interaction of ambient seawater with the anoxic pore fluids and unstable siliceous and carbonate debris within the sediment. The staining by glauconite of all the surfaces of this hardground in contact with the Chalk sea gives an indication of the extent of the transformations and neoformations that may have occurred in the development of the Chalk's smectite assemblage.

The Campanian sequence of chalk, flint and thin marls at Peacehaven displays cryptic anoxic cementation that must have developed some way below the water/sediment interface. The variable degrees of cementation and the variation in the heating behaviour of the smectite assemblage (Jeans *et al.*, 2014) could be related to the development of smectite under changing cation populations associated with periods of anoxic cementation.

ACKNOWLEDGMENTS

We wish to thank the following: Vivien Brown and Philip Stickler respectively for help in preparing the manuscript and figures; Michael Hall and James Rolfe for stable isotope analysis; Chiara Petroni for electron microprobe analysis; Rory Mortimore for much stratigraphical guidance and help in sample collecting at Peacehaven as well as for the aerial photograph; Tony Dickson for his unrivalled carbonate expertise and unstinting help; Tony Fallick, Alex Brasier and Mark Wilkinson for their helpful comments and suggestions; the Chinese Science Council and the Department of Earth Sciences respectively for financial support and hospitality during X.F. Hu's visit (2009–10) to Cambridge.

REFERENCES

- Bower C.R. & Farmery J.T. (1910) The zones of the Lower Chalk of Lincolnshire. *Proceedings of the Geologists' Association*, **11**, 333–359.
- Bräutigam F. (1962) *Zur Stratigraphie und Paläontologie des Cenomans und Turons im Nordwestlichen Harzvorland*. PhD thesis, Universität Braunschweig, Germany.
- Deconinck J.F. & Chamley H. (1995) Diversity of smectite origins in Late Cretaceous sediments: Examples of chalks from northern France. *Clay Minerals*, **30**, 365–379.
- Deconinck J.F., Amédéo F., Baudin F., Godet A., Pellenard P., Robaszynski F. & Zimmerlin I. (2005) Late Cretaceous palaeoenvironments expressed by the clay mineralogy of Cenomanian–Campanian chalks from the east of the Paris Basin. *Cretaceous Research*, **26**, 171–179.
- Dickson J.A.D. & Barber C. (1976) Petrography, chemistry and origin of early diagenetic concretions in the Lower Carboniferous of the Isle of Man. *Sedimentology*, **23**, 189–211.
- Dorn P. & Bräutigam F. (1959) Hinweise auf Oberkreidevulkanismus in NW-Deutschland. *Abhandlungen der Braunschweigischen Wissenschaftlichen Gesellschaft*, **11**, 1–4.
- Duplaix S., Dupuis J., Camez T., Lucas J. & Millot J. (1960) Sur la nature des minéraux argileux inclus dans les calcaires sénoniens de l'Angoumois. *Bulletin du Service de la carte géologique d'Alsace et de Lorraine*, **13**, 157–162.
- Hardman R.F.P. (1982) Chalk reservoirs of the North Sea. *Bulletin of the Geological Society of Denmark*, **30**, 119–137.
- Heim D. (1957) Über die mineralischen, nicht-karbonatische Bestandteile des Cenoman und Turon der mitteldeutschen Kreidemulden und ihre Verteilung. *Heidelberger Beiträge zur Mineralogie und Petrographie*, **5**, 302–330.
- Hendry J.P., Pearson M.J., Trewin N.H. & Fallick A.E. (2006) Jurassic septarian concretions from NW Scotland record interdependent bacterial, physical and chemical processes of marine mudrock diagenesis. *Sedimentology*, **53**, 537–565.
- Hu X.F., Jeans C.V. & Dickson J.A.D. (2012) Geochemical and stable isotope patterns of calcite cementation in the Upper Cretaceous Chalk, UK: Direct evidence from calcite-filled vugs in brachiopods. *Acta Geologica Polonica*, **62**, 143–172.
- Jeans C.V. (1973) The Market Weighton Structure; tectonics, sedimentation & diagenesis during the Cretaceous. *Proceedings of the Yorkshire Geological Society*, **39**, 409–444.
- Jeans C.V. (1978) Silicifications and associated clay assemblages in the Cretaceous marine sediments of southern England. *Clay Minerals*, **13**, 101–126.
- Jeans C.V. (1980) Early submarine lithification in the Red Chalk and Lower Chalk of eastern England: a bacterial control model and its implications. *Proceedings of the Yorkshire Geological Society*, **43**, 81–157.
- Jeans C.V. (2006) Clay mineralogy of the British Cretaceous. *Clay Minerals*, **41**, 47–150.

- Jeans C.V., Merriman R.J. & Mitchell J.G. (1977) Origin of the Middle Jurassic and Lower Cretaceous Fuller's earths in England. *Clay Minerals*, **12**, 11–44.
- Jeans C.V., Long D., Hall M.A., Bland D.J. & Cornford C. (1991) The geochemistry of the Plenus Marls at Dover, England: evidence of fluctuating oceanographic conditions and of glacial control during the development of the Cenomanian-Turonian $\delta^{13}\text{C}$ anomaly. *Geological Magazine*, **128**, 604–632.
- Jeans C.V., Fallick A.E., Fisher M.J., Merriman R.J., Corfield R.M. & Manighetti B. (1997) Clay- and zeolite-bearing Triassic sediments at Kaka Point: evidence of microbially influenced mineral formation from earliest diagenesis into the lower grades of metamorphism. *Clay Minerals*, **32**, 373–423.
- Jeans C.V., Hu X.F. & Mortimore R.N. (2012) Calcite cements and the stratigraphical significance of the marine $\delta^{13}\text{C}$ carbonate reference curve for the Upper Cretaceous Chalk of England. *Acta Geologica Polonica*, **62**, 173–196.
- Jeans C.V., Tosca N.J., Boreham S. & Hu X.F. (2014) Clay mineral-grain size-calcite cement relationships in Upper Cretaceous Chalk, UK: a preliminary investigation. *Clay Minerals*, **49**, 299–325.
- Lindgreen H., Drits V.A., Sakharov B.A., Jakobsen H.J., Salyn A.L., Dainyat L.G. & Krøyer H. (2002) The structure and diagenetic transformation of illite-smectite and chlorite-smectite from North Sea Cretaceous–Tertiary chalk. *Clay Minerals*, **37**, 429–450.
- Lindgreen H., Drits V.A., Jakobsen F. & Sakharov B.A. (2008) Clay mineralogy of the central North Sea Upper Cretaceous-Tertiary chalk and the formation of clay-rich layers. *Clay and Clay Minerals*, **56**, 693–710.
- Maliva R.G. & Dickson J.A.D. (1997) Ulster White Limestone Formation (Upper Cretaceous) of Northern Ireland: effects of basalt loading on chalk diagenesis. *Sedimentology*, **44**, 105–112.
- Millot G. (1949) Relations entre la constitution et la genèse des roches sédimentaires argileuses. *Thèse Science Nancy, Géologie Appliquée et Prospection Minière*, **2**, 352 pp.
- Millot G. (1964) *Géologie des Argiles*, Masson et Cie, Paris, 500 pp.
- Millot G., Camez T. & Bonte A. (1957) Sur la montmorillonite dans les craies. *Bulletin du Service de la carte géologique d'Alsace et de Lorraine*, **10**, 25–26.
- Mitchell S.F. (1995) Lithostratigraphy and biostratigraphy of the Hunstanton Formation (Red Chalk, Cretaceous) succession at Speeton, North Yorkshire, England. *Proceedings of the Yorkshire Geological Society*, **50**, 285–303.
- Mitchell S.F. (1996) Foraminiferal assemblages from the late Lower and Middle Cenomanian of Speeton (North Yorkshire, UK): relationships with sea-level fluctuations and watermass distribution. *Journal of Micropalaeontology*, **15**, 37–54.
- Mortimore R.N. (1986) Stratigraphy of the Upper Cretaceous White Chalk of Sussex. *Proceedings of the Geologists' Association*, **97**, 97–139.
- Mortimore R.N. (2012) Making sense of Chalk: a total rock approach to its engineering geology. *Quarterly Journal of Engineering Geology and Hydrology*, **45**, 252–334.
- Raiswell R. (1971) The growth of Cambrian and Liassic concretions. *Sedimentology*, **17**, 147–171.
- Raiswell R. (1976) The microbiological formation of carbonate concretions in the Upper Lias of NE England. *Chemical Geology*, **18**, 227–244.
- Schöner H. (1960) Über die Verteilung und Neubildung der nichtkarbonatischen Mineralkomponenten der Oberkreide aus der Umgebung von Hannover. *Beiträge zur Mineralogie und Petrographie*, **7**, 76–103.
- Valeton I. (1959) Eine vulkanische Tufflage aus der Oberkreide von Hemmoor/Niederelbe. *Neues Jahrbuch für Geologie und Paläontologie*, 193–204.
- Valeton I. (1960) Vulkanische tuffteineinlagerung in der nordwestdeutschen Oberkreide. *Mitteilungen aus dem Geologischen Staatsinstitut in Hamburg*, **29**, 26–41.
- Weir A.H. & Catt J.A. (1965) The mineralogy of some Upper Chalk samples from the Arundel area, Sussex. *Clay Minerals*, **6**, 97–110.
- Wood C.J. & Smith E.G. (1978) Lithostratigraphical classification of the Chalk in North Yorkshire, Humberside and Lincolnshire. *Proceedings of the Yorkshire Geological Society*, **42**, 263–287.
- Wray D.S. (1995) Origin of clay-rich beds in Turonian chalks from Lower Saxony, Germany: a rare earth element study. *Chemical Geology*, **119**, 161–173.
- Wray D.S. (1999) Identification and long-range correlation of bentonites in Turonian-Coniacian (Upper Cretaceous) chalks of northwest Europe. *Geological Magazine*, **136**, 361–371.
- Wray D.S. & Wood C.J. (1995) Geochemical identification and correlation of tuff layers in Lower Saxony, Germany. *Berliner Geowissenschaftliche Abhandlungen*, **E16.1**, 215–226.
- Wray D.S. & Wood C.J. (1998) Distinction between detrital and volcanogenic clay-rich beds in Turonian-Coniacian chalks of eastern England. *Proceedings of the Yorkshire Geological Society*, **52**, 95–105.
- Wray D.S., Kaplan U. & Wood C.J. (1995) Tuff-Vorkommen und ihre bio- und eventstratigraphie im Turon des Teutoburger Waldes, der Egge und des Haarstrangs. *Geologie und Paläontologie in Westfalen*, **37**, 1–53.
- Wray D.S., Wood C.J., Ernst G. & Kaplan U. (1996) Geochemical subdivision and correlation of clay-rich beds in Turonian sediments of northern Germany. *Terra Nova*, **8**, 603–610.